Thesis for the Degree of Licentiate of Engineering

Robust Transceiver Design and Waveform Synthesis for Wideband MIMO Radar

Marie Ström

Department of Signals and Systems
Chalmers University of Technology
Göteborg, Sweden 2012

Robust Transceiver Design and Waveform Synthesis for Wideband MIMO Radar

Marie Ström

Technical report number: R009/2012
ISSN 1403-266X

Department of Signals and Systems
Chalmers University of Technology
SE–412 96 Göteborg
Sweden
Telephone: +46 (0)31 – 772 1000

Typeset by the author using LaTeX.

Chalmers Reproservice
Göteborg, Sweden 2012

To my sister, Anna

Abstract

This thesis deals with the problem of designing and synthesizing waveforms that are optimal, both in a signal-to-noise-and-interference ratio (SNIR), and in a system hardware design perspective, i.e., to synthesize time domain waveforms with a low peak-to-average power ratio (PAPR), or even constant modulus.

In the first part of the thesis, we investigate the possibility to suppress interference for wideband multiple-input multiple-output radar, by exploiting the spectral properties of the transmit signals. The idea is to use tunable filters at the transmitter and receiver sides, and to derive the optimal power spectral density that enhances the system performance in terms of the SNIR, for a given scenario. Herein, the focus is to suppress active jamming interference, and especially deceptive jamming. The proposed method is extended to invoke imperfections in the given scenario. Two robust optimization methods are evaluated: one that utilizes a Taylor series expansion of the SNIR, and one that exploits a worst-case SNIR maximization.

In the second part of the thesis, we utilize the results obtained in the first part to synthesize time domain signals that achieve certain hardware restrictions. By using the technique of partial transmit sequence, we synthesize signals that achieve optimal spectral properties and that experience a low PAPR. Finally, we show that if we allow the power spectrum to deviate somewhat from its desired shape, a further reduction of the PAPR, or even a constant modulus signal is possible. The proposed method can be used to design a time domain signal with any predefined power spectrum, if there is no design restriction except for the PAPR on the time domain signal waveform.

Keywords: MIMO radar, Wideband radar, Transmit–receive filter design, Robust analysis, Interference, Waveform synthesis

Acknowledgments

I would like to take the opportunity to thank some very special people, without their help this thesis would never have been written. First and foremost, I would like to thank my supervisor Professor Mats Viberg, for accepting me as a Ph.D. student, for believing in me, and for all the support you have given me during these first years.

Next, I would like to thanks my co-supervisor Kent Falk at Saab EDS, for much needed guidance in both theoretical and practical knowledge of radar systems. A special thanks to Johan Carlert, who accepted me as an Industrial Ph.D student at Saab EDS in January 2012. I look forward spending many years working at Saab EDS.

Obviously, gratefully acknowledged is the received funding from the Swedish Research Council (VR).

There are a number of people at the the Department of Signals and Systems who deserve a special thanks. The administrate staff for helping out with all non-technical issues, and Lars for computer related support. Also, everyone at the Signal Processing group is acknowledged, for giving me an enjoyable working environment.

I would also like to show my gratitude to my closest friends: Charlotta, Louise, Ulrika, Lina, Jenni, Eija, Irena, Henrik, and Thomas. Next, I would like to express my deepest love to my mother Gunilla, my father Gunnar, and their partners Stefan and Aina. Foremost, I would like to thank my sister Anna for all the great support and encouragement during many years. I know that I would never have been able to go this far without my families' and friends' help when I desperately needed it. The one thing that I will always be sure of, is that they will always be there for me.

Last but not least, I would like to thank Daniel for being the most wonderful person in the world.

Marie Ström
Göteborg, June 2012

List of Publications

This thesis is based on the following two appended papers:

Paper 1

M. Ström, M. Viberg, and K. Falk, Robust Transceiver Design for Wideband MIMO Radar utilizing a Subarray Antenna Structure, To be submitted to *Special Issue on Advances in Sensor Array Processing, EURASIP Signal Processing Journal*.

Paper 2

M. Ström and M. Viberg, Low PAPR Waveform Synthesis with Application to Wideband MIMO Radar, *Proc. of the 4th International Workshop on Computational Advances in Multi-Sensor Adaptive Processing* , December 2011, San Juan, Puerto Rico.

Other Publications

M. Ström, M. Viberg, and K. Falk, Transmit and Receive Filter Optimization for Wideband MIMO Radar, *Proc. of the 4th International Workshop on Computational Advances in Multi-Sensor Adaptive Processing* , December 2011, San Juan, Puerto Rico.

E. Johansson, M. Ström, L. Svensson and M. Viberg, Interpolation based on stationary and adaptive AR(1) modeling, *IEEE International Conference on Acoustics, Speech, and Signal Processing*, May 2011, Prague, Czech Republic.

M. Ström, E. Johansson, and D. Stork, Mapping Colors from Paintings to Tapestries: Rejuvenating the Faded Colors in Tapestries based on Colors in Reference Paintings, *SPIE Electronic Imaging: Human Vision and Electronic Imaging XVII*, January 2012, San Fransisco, USA

M. Ström and M. Viberg, Constant Modulus Waveform Synthesis with Application to Wideband MIMO Radar, *Conference Presentation at Swedish Radio and Microwave Days*, March 2012, Stockholm, Sweden

Contents

Abstract **i**

Acknowledgments **iii**

List of Publications **v**

Contents **vii**

I Introductory Chapters

1 Introduction **1**
1.1 Contributions 3
1.2 Outline 3

2 Introduction to Radar **5**
2.1 Radar Signal Basics 5
2.2 Radar Detection Fundamentals 6
2.3 Antenna Array Beamforming 11
2.3.1 Wideband Antenna Arrays 13
2.4 Radar Scenario 16

3 Robust Transceiver Optimization and Waveform Synthesis **19**
3.1 MIMO Radar 19
3.1.1 Waveform Design Utilizing the Spatial Properties of the Transmitted Signals 21
3.1.2 Waveform Design Utilizing the Temporal Properties of the Transmitted Signals 21
3.2 Robust Analysis 24
3.3 Waveform Synthesis 25

4 Summary of Appended Papers **29**

5 Conclusions and Future Work **31**
5.1 Conclusions 31
5.2 Future Work 32

References **35**

II Included Papers

Paper 1 Robust Transceiver Design for Wideband MIMO Radar utilizing a Subarray Antenna Structure **45**
1 Introduction 45
2 System Model 49
3 SNIR Maximization 53
3.1 Alternating Transmit–Receive Filter Optimization . . 54
3.2 Joint Transmit–Receive Filter Optimization 55
4 Robustness to Mismatch Errors of the Spatial Position . . . 56
4.1 Taylor Series Expansion of the SNIR 57
4.2 Worst-Case SNIR Maximization 59
5 Numerical Validation 59
5.1 Experiment 1: Alternating versus Joint Transmit–Receive Filter Optimization 60
5.2 Experiment 2: Adaptive Filters versus non-Adaptive Filters 62
5.3 Experiment 3: Robustness Analysis 63
6 Concluding Remarks and Discussion 64
References 68

Paper 2 Low PAPR Waveform Synthesis with Application to Wideband MIMO Radar **75**
1 Introduction 75
2 Problem Formulation 77
3 Waveform Synthesis 77
4 Relation to Previous Work 79
5 Experimental Validation 79
6 Conclusions 82
References 83

Part I

Introductory Chapters

Chapter 1

Introduction

The strive of mankind to develop new technologies most certainly started the day the first human set foot on Earth. Now, eons later, our society still advocate the necessity for new products. In this thesis, we discuss a rather new technology, nowadays so acknowledged that the abbreviation is a commonly known word, namely **radar**, or **ra**dio **d**etection **a**nd **r**anging. What makes this technology so popular in the society? – Probably its usability in various applications. We encounter radar in systems ranging from active safety systems for cars and trucks, through medical applications, such as cancer treatment, to military and civil surveillance.

From a historical perspective, the demonstration of the similarity between radio waves and light, conducted by Heinrich Hertz in the late 19th century, is generally seen as the start of the great advances in the area of remote sensing. Hertz provided the world with the knowledge of reflection on metallic surfaces, as well as refraction in dielectric prisms for radio waves. Hertz' research was advanced by Christian Hülsmeyer, who in 1904 obtained the first patent for a radar system that detected ships. However, mankind was not ready for such a new and advanced technology, so it slowly faded into people's memories. However, in the 1920s, Gugliermo Marconi advocated these ideas, and his speech delivered before the Institute of Radio Engineers, might be seen as the startup of the great development in radar technology. The research accelerated and spread throughout the world during the rest of the 20th century, mostly due to its use in military operations [1, 2].

It is probably impossible, and not fair at all, to order the importance of developed for radar techniques. However, there are four great advances that significantly improved the radar system performance, namely

- the invention of the high-power microwave magnetron
- the use of the Doppler effect

- the technology of pulse compression
- the electronically steered phased array.

Today, there is a hope among researchers that the so-called multiple-input multiple-output (MIMO) radar will be the next item on the list of great advances. MIMO antenna systems first appeared for communication applications, where the system performance was dramatically improved [3]. However, the underlying problems and objectives are quite different in communication and radar. Nonetheless, research so far have shown that a MIMO antenna configuration for radar can improve, for instance, the target identifiability, and the resolution of the target's location [4, 5]. It is also anticipated that MIMO radar will experience an improvement in difficult environments, which involve strong clutter and jamming, compared with traditional radar.

When transmitting multiple arbitrary waveforms, electronic surveillance equipment with classical libraries of frequencies, pulse repetition intervals, and pulse lengths might become obsolete. Moreover, the possibility to design waveforms that improve the stealth properties of the radar arises, meaning that the radar will be more difficult to discover compared with the waveforms used nowadays.

Research on wideband systems has been a trend in hardware design for several decades. However, traditional radar detection theory has to a great extent focused on narrowband systems. The situation that arises is that highly flexible wideband transmitters are available, but it is not well understood how they should be used.

In this thesis, we combine the idea of using multiple waveforms with a wideband system. The multiple waveforms are simultaneously transmitted from different antennas, or groups of antennas, i.e., MIMO radar. To design and adapt the waveforms, we employ tunable filters at the transmitter and receiver sides, respectively, and seek the optimal filter coefficients that increase the system performance, measured as the signal-to-noise-and-interference ratio (SNIR), under the given prevailing conditions. The results are extended to incorporate imperfections in the given scenario. The maximization of the SNIR is performed in the frequency domain, and as several time domain waveforms experience the same spectral properties, we seek to synthesize waveforms that also experience desirable time domain properties. This is an important and fundamental interest in a broad variety of applications, and in this thesis we focus on the design of time domain signals that experience a low peak-to-average-power ratio (PAPR), or even a constant envelope.

1.1 Contributions

The main contributions of this thesis are:

- Optimal design of transmit and receive filters for wideband MIMO radar given a known scenario.
- Robust optimal design of the transmit filters invoking imperfections in the given scenario.
- Synthesis of wideband time domain waveforms with a low PAPR, or a constant envelope.

1.2 Outline

The thesis consists of two parts. Part I contains background information to explain the context of the appended papers. Part II contains two scientific papers that constitute the base for the thesis. A bibliography is included at the end of Part I, and after each paper in Part II.

In Part I, Chapter 2 provides a short introduction to radar basics, detection, beamforming, and the radar scenario. Chapter 3 contains an overview of the robust transmit–receive filter design, and the synthesis of the actual waveforms. A summary of the papers is given in Chapter 4. Part I is ended with conclusions and future work in Chapter 5.

Chapter 2

Introduction to Radar

The purpose of this chapter is to provide a very short introduction to radar fundamentals; for a comprehensive study, see, e.g., the books [1, 2, 6].

The main purpose of a radar system is the *detection*, *tracking*, and possibly, *imaging*, *identification*, and *classification* of objects contained in the environment of operation. In this thesis, we are only interested in the detection properties. Henceforth, tracking, imaging, identification, and classification will not be discussed.

This chapter is divided into four sections, where we cover four basic concepts of radar signal processing: first, a short introduction to the transmitted radar signals, thereafter, detection fundamentals followed by beamforming for narrowband and wideband systems, and last an explanation of the objects included in a radar scenario.

2.1 Radar Signal Basics

Consider a radar system that transmits a series of pulses, namely, a pulsed radar [1]. For a traditional radar system, utilizing no pulse compression, each pulse contains a narrowband signal modulated on a carrier. One of the transmitted pulses is modeled as

$$v(t) = a(t)e^{j(2\pi f_0 t - \psi(t))}. \tag{2.1}$$

In (2.1), f_0 is the carrier frequency, $a(t)$ the pulse shape, and $\psi(t)$ is the phase modulation. Assume that one pulse has a duration of τ seconds. The duration of the pulse specifies the quantity called range resolution, and for an unmodulated, constant frequency pulse the range resolution is $\Delta R = \frac{c\tau}{2}$, where c is the speed of light in the medium of propagation. Thus, scatterers contained within the range ΔR contributes to the received voltage. The received signal from a single scatter point at the distance $R = \frac{ct_0}{2}$, t_0 being

the time delay, is expressed as

$$\tilde{v}(t) = \tilde{a}(t - t_0)e^{j(2\pi f_0(t-t_0)-\tilde{\psi}(t))} + n(t), \tag{2.2}$$

where $\tilde{a}(t)$ is the echo amplitude, $\tilde{\psi}(t)$ the echo phase modulation, and $n(t)$ the receiver noise. In general, $\tilde{a}(t)$ is much smaller than $a(t)$, and often also smaller than the noise level [2]. Thus, detecting the presence (or not) of a target requires some filtering operations, and a good detector. After the pulse, or pulse train, is received, there are several different signal processing steps applied to the measurements. *Fast time* operations are applied to a single pulse, e.g., beamforming, sampling, and matched filtering. In comparison, *slow time* operations, which are applied to the complete pulse train are, e.g., Doppler processing and space-time adaptive processing.

2.2 Radar Detection Fundamentals

The incoming signal at the receiver antenna array is first passed through a band-pass filter, and a low noise amplifier (LNA), which increases the amplitude of the signal echo. Throughout this section, the target echo is not corrupted by interference. Thus, the noise contributions are generated at the receiver only. We investigate the performance of a classical coherent receiver that employs a threshold detector, see Figure 2.1 for a block diagram of the receiver. For a coherent receiver, one expects that the signal

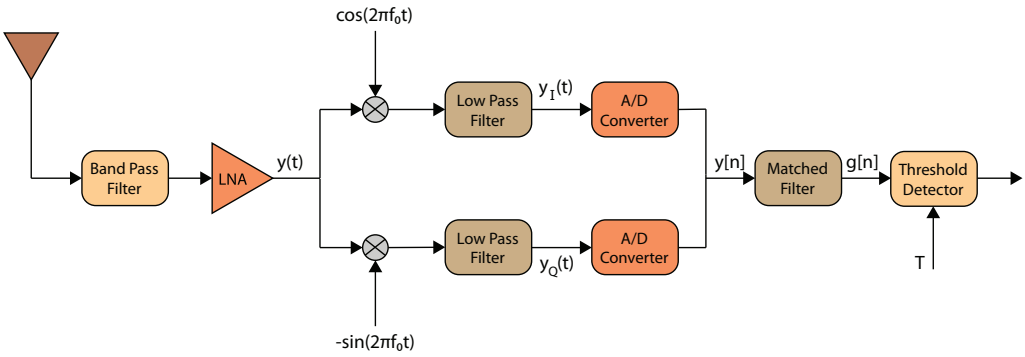

Figure 2.1: Block diagram of a classical coherent receiver utilizing a threshold detector.

echoes from N samples are deterministic, and therefore, by integrating over the samples we can retain the phase information. This is called *coherent integration*. In comparison, if the data first has to be preprocessed to align the phases of the received samples, a noncoherent receiver and *noncoherent integration* are employed. This happens, for instance, when the target is

moving, and the measured signal component experiences a so-called *Doppler shift*. Noncoherent integration is not in the scope of this introduction, and the reader is instead referred to [1].

The output signal from the band-pass filter and the LNA, here denoted $y(t)$, is expressed as

$$y(t) = r(t)\cos(2\pi f_0 t - \phi(t)) + n(t), \tag{2.3}$$

where $r(t)$ is the amplified received signal amplitude and $n(t)$ is the receiver noise, which is modeled as a complex zero-mean circular random process with variance σ_n^2. The in-phase (I) and quadrature (Q) signal components are, respectively,

$$\begin{aligned} y_I(t) &= r(t)\cos\phi(t) + n_Q(t), \\ y_Q(t) &= r(t)\sin\phi(t) + n_I(t). \end{aligned} \tag{2.4}$$

In (2.4), $\phi(t) = \arctan(y_Q(t)/y_I(t))$, and for simplicity the possible scaling factor due to the low-pass filter is omitted. The signal is sampled at $t = nT_s$, where $T_s = \frac{1}{B}$, B being the bandwidth of the system. The resulting complex digital signal is

$$y[n] = y_I(nT_s) + jy_Q(nT_s). \tag{2.5}$$

The sampled signal sequence is $\mathbf{y} = \begin{bmatrix} y[0] & y[1] & \dots & y[N-1] \end{bmatrix}^T$, where N is the length of the signal. Our goal is to detect if a target is present by investigating the measured signal $\mathbf{y}$. The predefined assumption that the signal echo is not corrupted by interference leads to that $\mathbf{y}$ contains either a signal echo and receiver noise, or receiver noise only. Therefore, the ability of the radar receiver to detect an echo is limited by the level of noise in the receiver system.

Detection theory for radar analysis is an example of a binary decision problem, where we seek to detect if a signal is present or absent. Hence, we investigate the two hypotheses:

$$\begin{aligned} \mathcal{H}_1 &: \mathbf{y} = \mathbf{s} + \mathbf{n} \sim \mathcal{N}(\mathbf{r}, \sigma_n^2\mathbf{I}), \\ \mathcal{H}_0 &: \mathbf{y} = \mathbf{n} \sim \mathcal{N}(\mathbf{0}, \sigma_n^2\mathbf{I}). \end{aligned} \tag{2.6}$$

For an ideal detector, we always choose $\mathcal{H}_1$ if a target is present, and $\mathcal{H}_0$ if a target is absent. However, this is not the case in reality. There are two kinds of errors that might occur. First, we might decide that a signal is present when it is not, i.e., we produce a false alarm, and second that we decide that a signal is absent when it is not, i.e., a missed detection. The probability of a false alarm and a miss detection are denoted P_{fa} and P_m, respectively. The probability of detecting a signal is $P_d = 1 - P_m$.

For the radar system engineer, the acceptable P_{fa} is typically given by an acceptable error rate, and we seek to maximize the P_d. This problem results in the so-called *Neyman-Pearson lemma*.

Define $p(\mathbf{y}|\mathcal{H}_1)$ and $p(\mathbf{y}|\mathcal{H}_0)$ as the conditional probability density functions (pdfs) of the received signal given a target and no target, respectively. At the detector a likelihood ratio test (LRT) is performed, which is defined as

$$\mathcal{L}(\mathbf{y}) = \frac{p(\mathbf{y}|\mathcal{H}_1)}{p(\mathbf{y}|\mathcal{H}_0)} \underset{\mathcal{H}_0}{\overset{\mathcal{H}_1}{\gtrless}} \lambda, \tag{2.7}$$

where λ is a threshold related to the acceptable P_{fa}. A convenient, common notation is instead to express the LRT as its equivalent *log-likelihood ratio*, i.e.,

$$\ln \mathcal{L}(\mathbf{y}) \underset{\mathcal{H}_0}{\overset{\mathcal{H}_1}{\gtrless}} \ln \lambda. \tag{2.8}$$

By invoking the characteristics of the target signal and the receiver noise, as described in (2.6), we express the conditional pdfs $p(\mathbf{y}|\mathcal{H}_1)$ and $p(\mathbf{y}|\mathcal{H}_0)$ of N complex samples as, respectively,

$$\begin{aligned} p(\mathbf{y}|\mathcal{H}_1) &= \frac{1}{\pi^N \sigma_n^{2N}} e^{-\frac{(\mathbf{y}-\mathbf{r})^H(\mathbf{y}-\mathbf{r})}{\sigma_n^2}}, \\ p(\mathbf{y}|\mathcal{H}_0) &= \frac{1}{\pi^N \sigma_n^{2N}} e^{-\frac{\mathbf{y}^H\mathbf{y}}{\sigma_n^2}}. \end{aligned} \tag{2.9}$$

Inserting (2.9) into (2.8) gives the log-likelihood ratio as

$$\ln \mathcal{L}(\mathbf{y}) = \frac{1}{\sigma_n^2}\left(2\Re(\mathbf{r}^H\mathbf{y}) - \mathbf{r}^H\mathbf{r}\right). \tag{2.10}$$

Here, $\Re(\cdot)$ is the real part, and the product $\mathbf{r}^H\mathbf{y}$ is the output from a so-called *matched filter*, when the vector $\mathbf{y}$ and the impulse response $\mathbf{r}$ completely overlap, since $\mathbf{r}$ is the impulse response of the signal that is supposed to be detected under the hypothesis $\mathcal{H}_1$. Here, $\mathbf{r}$ is the mean of the signal to be detected. However, the elements in $\mathbf{r}$ can be samples of the transmitted modulated waveform, or any other function of interest. From (2.10), it is seen that the likelihood ratio is only a function of the term $\Re(\mathbf{r}^H\mathbf{y})$, which determines the outcome of the test. This data dependent term is called a *sufficient statistic*, and is in this situation expressed as

$$\Upsilon(\mathbf{y}) = \Re(\mathbf{r}^H\mathbf{y}) = \Re\left\{\sum_{n=0}^{N-1} r[n]^C y[n]\right\}, \tag{2.11}$$

where $(\cdot)^C$ denotes the complex conjugate. Expressing the LRT with the sufficient statistic results in

$$\Upsilon(\mathbf{y}) \underset{\mathcal{H}_0}{\overset{\mathcal{H}_1}{\gtrless}} T. \tag{2.12}$$

Here, T is the threshold for the sufficient statistic. The sufficient statistic is a sum of Gaussian random variables, which will also be Gaussian.

To evaluate the performance of the detector, we need to determine the pdf of Υ under the hypotheses. First, introduce the scalar $g = \mathbf{r}^H\mathbf{y}$, which is a complex Gaussian random variable. We start with the investigation of the hypothesis $\mathcal{H}_0$, and note that $y[n]$ are independent and zero-mean as no signal is present. Thus, the variance of g under $\mathcal{H}_0$ is

$$\mathrm{E}[\mathbf{r}^H\mathbf{y}\mathbf{y}^H\mathbf{r}] = NA^2\sigma_n^2, \tag{2.13}$$

where A^2 is the energy of one sample in the impulse response $\mathbf{r}$. The matched filter output is therefore distributed as $g \sim \mathcal{N}(0, NA^2\sigma_n^2)$. Continuing, under the hypothesis $\mathcal{H}_1$, the random variable g is instead distributed as $g \sim \mathcal{N}(NA^2, NA^2\sigma_n^2)$, assuming a non fluctuating target. The sufficient statistic (2.11) is the real part of g. The mean of g is real, and the power of a complex Gaussian divides equally between the real and imaginary parts of the random variable g [7]. Thus,

$$\begin{aligned} \mathcal{H}_1: &\quad \Upsilon \sim \mathcal{N}(NA^2, NA^2\frac{\sigma_n^2}{2}), \\ \mathcal{H}_0: &\quad \Upsilon \sim \mathcal{N}(0, NA^2\frac{\sigma_n^2}{2}). \end{aligned} \tag{2.14}$$

Note that the notation $\mathcal{N}((\cdot),(\cdot))$ is used both for complex and real distributions. From (2.12), a false alarm occurs if $\Upsilon \geq T$ under the hypothesis $\mathcal{H}_0$. Hence, the P_{fa} is calculated as

$$\begin{aligned} P_{fa} &= \int_T^\infty p(\Upsilon|\mathcal{H}_0)d\Upsilon = \int_T^\infty \frac{1}{\sqrt{\pi NA^2\sigma_n^2}} e^{-\frac{\Upsilon^2}{NA^2\sigma_n^2}} d\Upsilon = \\ &= \frac{1}{2}\left[1 - \mathrm{erf}\left(\frac{T}{\sqrt{NA^2\sigma_n^2}}\right)\right]. \end{aligned} \tag{2.15}$$

In (2.15), $\mathrm{erf}(\cdot)$ is the *error function*, and its definition can be found in [8]. Generally, it is convenient to invert (2.15) to obtain the threshold $T = \sqrt{NA^2\sigma_n^2}\mathrm{erf}^{-1}(1-2P_{fa})$, which achieves a predefined P_{fa}. To derive the P_d,

we instead investigate

$$P_d = \int_T^\infty p(\Upsilon|\mathcal{H}_1)d\Upsilon = \int_T^\infty \frac{1}{\sqrt{\pi NA^2\sigma_n^2}} e^{-\frac{(\Upsilon - NA^2)^2}{NA^2\sigma_n^2}} d\Upsilon = \tag{2.16}$$
$$= \frac{1}{2}\left[1 - \text{erf}\left(\frac{T - NA^2}{\sqrt{NA^2\sigma_n^2}}\right)\right].$$

Inserting $T = \sqrt{NA^2\sigma_n^2}\text{erf}^{-1}(1 - 2P_{fa})$ into (2.16) gives the probability of detection with respect to P_{fa}, as

$$P_d = \frac{1}{2}\left[1 - \text{erf}\left(\frac{\sqrt{NA^2\sigma_n^2}\text{erf}^{-1}(1 - 2P_{fa}) - NA^2}{\sqrt{NA^2\sigma_n^2}}\right)\right] = \tag{2.17}$$
$$= \frac{1}{2}\text{erfc}\left(\text{erf}^{-1}\left(1 - 2P_{fa}\right) - \sqrt{\frac{NA^2}{\sigma_n^2}}\right).$$

Here, $\text{erfc}(\cdot) = 1 - \text{erf}(\cdot)$ is the *complementary error function* and $\text{erf}^{-1}(\cdot)$ is the inverse error function. In (2.17), the term $\frac{A^2}{\sigma_n^2}$ is the signal-to-noise ratio (SNR), and as seen the P_d depends on this ratio. Note that the number of samples for one pulse, N, is introduced as a coherent gain. In Figure 2.2, the pdfs for the sufficient statistic under the hypotheses $\mathcal{H}_1$ and $\mathcal{H}_0$ are depicted. The picture also gives an illustrative interpretation of the threshold's impact on the P_m and P_{fa}.

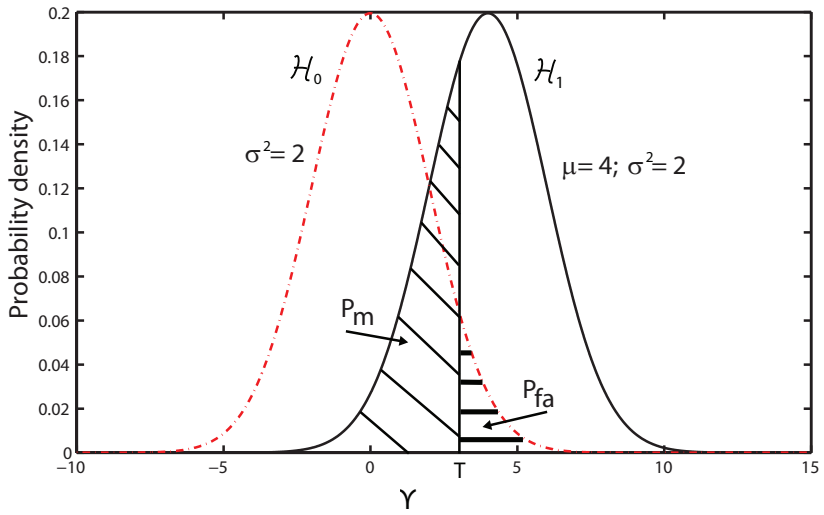

Figure 2.2: Probability density functions for the sufficient statistic under the hypotheses $\mathcal{H}_1$ and $\mathcal{H}_0$.

When designing a radar system, typically the minimum allowable SNR and the P_{fa} specifies the P_d. The performance of a detector is commonly

evaluated by the receiver operating characteristics (ROC) curves, see Figure 2.3, where the P_d for a given P_{fa} is depicted for various values of the SNR. After the signal processing, for the system to work properly, a typ-

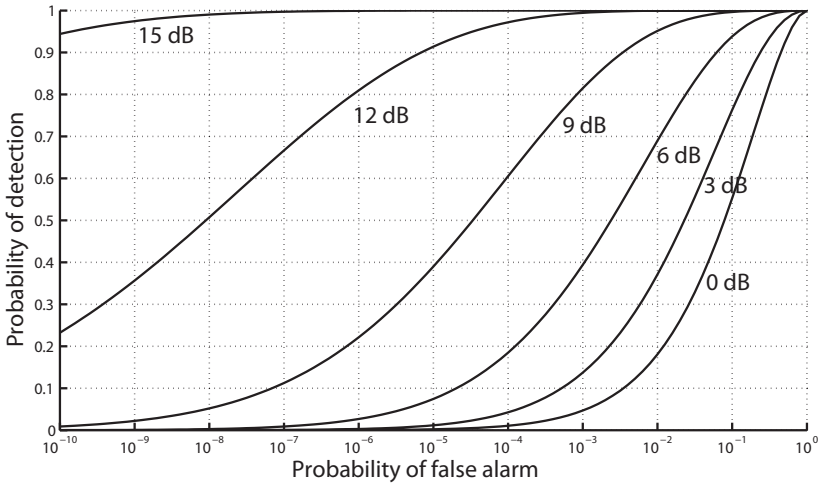

Figure 2.3: ROC curves, describing the performance of the detector in a classical coherent receiver, for several values of the SNR.

ical value of the SNR has to be above 10 dB, and a way to improve the performance in terms of P_d and P_{fa} is to increase the SNR.

For the calculations performed above, perfect knowledge of all parameters contained in the conditional pdfs $p(\Upsilon|\mathcal{H}_1)$ and $p(\Upsilon|\mathcal{H}_0)$ is assumed. Thus, perfect knowledge of $p(\mathbf{y}|\mathcal{H}_1)$ and $p(\mathbf{y}|\mathcal{H}_0)$ is required. Unfortunately, this is not the case in the real world. The situation that affects the structure of the detector the greatest is where the type of pdf is known (Gaussian Rayleigh, etc.), but where the parameters of the pdf are unknown and random [2]. Specifically, perfect knowledge of the impulse response, $\mathbf{r}$, is unrealistic. Instead, it is more reasonable to assume knowledge of $\mathbf{r}$ within an unknown phase factor $e^{j\theta}$, where θ is a random variable [2]. There are two ways to handle this situation. First, we can employ a *generalized likelihood ratio test* (GLRT), where the unknown phase and damping are replaced with their maximum likelihood estimates. Second, we can use the *Bayesian approach*, where we compute the pdfs under the hypotheses by separately averaging the conditional pdfs. A good introduction to the GLRT and the Bayesian approach can be found in [7].

2.3 Antenna Array Beamforming

The use of antenna arrays introduces the possibility to form directive beams, which if the signals are combined properly increases the strength of the

outgoing and incoming signals [9]. Herein, we first introduce antenna arrays and narrowband systems. The discussion is followed by a short introduction to wideband system models.

To transmit and receive signals, an array of sensors (antenna elements) are distributed over a surface. The purpose of the array is for example

- localization of a source
- reception of messages from another source
- imaging of the medium of propagation.

There are three commonly used sensor configurations: uniform linear arrays (ULA), uniform planar arrays (ULP), and uniform circular arrays (UCL) [10]. Herein, the focus is on a ULA antenna setup. Therefore, ULPs and UCLs will not be further discussed.

When utilizing an antenna array, the signal can either be transmitted or received from multiple antennas. Thus, the signal is built up by several outputs/inputs, and the goal is to transmit/receive a combination of signals in the best possible way. Investigating the receiver side (same idea is used at the transmitter side), the received signals at each element are only time delayed versions of each other. To steer the antenna array (*beamforming*), i.e., to form a directive gain in another direction than the broadside, *phase shifters* are mounted after each element. The setup of a ULA employing L antenna elements at the receiver side is depicted in Figure 2.4. As illus-

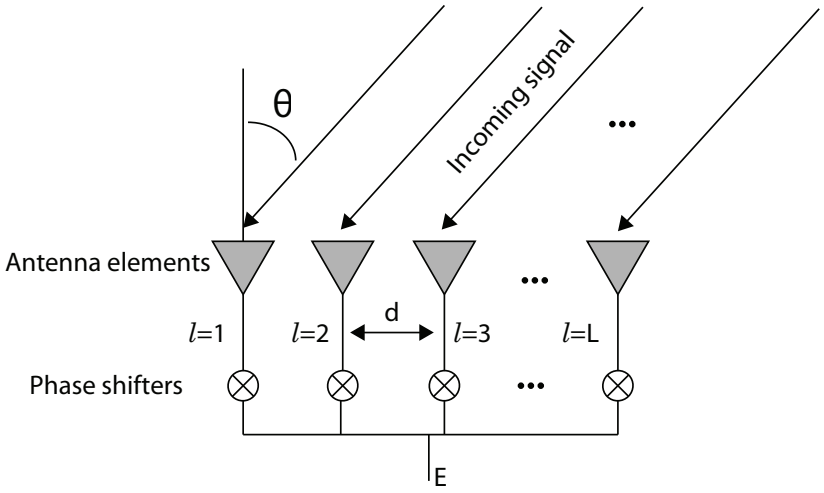

Figure 2.4: The geometry of a ULA with phase shifters that steer the directivity of the antenna array.

trated, the incoming signal arrives at the array from the angle θ. This angle

is commonly denoted the direction of arrival (DOA), and is measured with respect to the normal of the antenna array.

The time delay, which depends on the DOA, the inter-element spacing d, and the carrier frequency f_0 between the reference and the lth antenna element, is calculated as

$$\tau_l = \frac{dl \sin\theta}{c}. \tag{2.18}$$

To avoid the creation of grating lobes [1], typically $d \leq \frac{\lambda}{2}$, $\lambda = \frac{c}{f_0}$ being the wavelength at the frequency of operation. The time delay introduces a phase shift between the received signals at the antenna elements, and the output voltage E after the signal is combined at the phase shifters is

$$E = E_0 \sum_{l=0}^{L-1} w_l e^{j\omega_0 \tau_l} = E_0 \sum_{l=0}^{L-1} w_l e^{j\omega_0 \frac{dl}{c} \sin\theta}, \tag{2.19}$$

where E_0 contains the amplitude modulated incoming signal, and w_l is the applied phase shift for the lth antenna element. To maximize the energy, assuming uniform amplitude, the phase shifters are selected as

$$w_l = e^{-j\omega_0 \frac{dl}{c} \sin\alpha}\Big|_{\alpha=\theta}. \tag{2.20}$$

Here, α is the so-called the *steering angle*. Hence, to maximize the energy, the array is steered towards the DOA of the incoming signal. The magnitude of the antenna response describes the directivity, which is expressed as

$$\mathrm{AP}(\alpha) = \sum_{k=0}^{K-1} \left| e^{-j\omega_0 \frac{dk}{c} (\sin\alpha - \sin\theta)} \right|. \tag{2.21}$$

In Figure 2.5, the narrowband antenna array responses for arrays comprising $L = \{10, 20\}$ elements are depicted. As illustrated, by increasing the number of elements the directivity or *antenna gain* is increased. Moreover, the resulting main lobe gets narrower when employing more antenna elements.

In this section, we have investigated fixed phase shifters. However, the phase shifters can also be derived adaptively, i.e., *adaptive beamforming*, where the weight coefficients, w_l, are adapted to the prevailing conditions. When employing an adaptive beamformer configuration, the possibility to, for example, place a null towards the direction of a jammer or strong clutter arises. However, this is not in the scope of this thesis. The readers are instead referred to, e.g., [10–12], where comprehensive introductions to adaptive array signal processing are given.

2.3.1 Wideband Antenna Arrays

Now we focus on wideband antenna systems, and the challenges that appear when we increase the bandwidth of the system. For a wideband system we

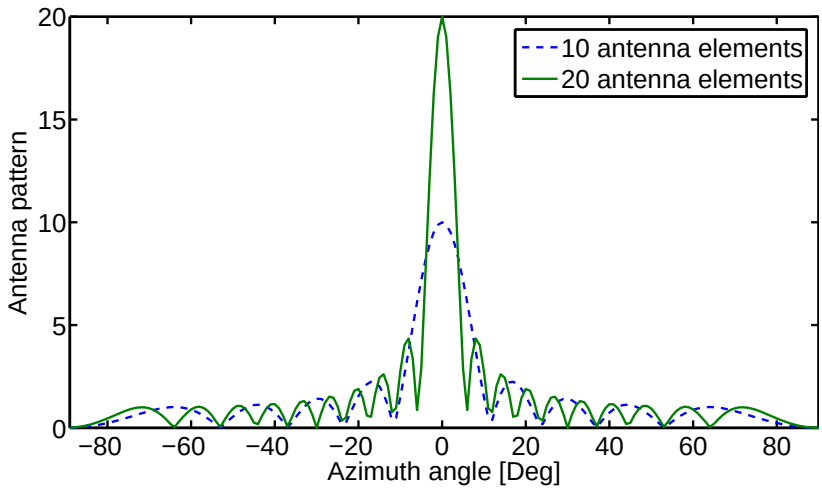

Figure 2.5: Antenna pattern for a ULA comprising 10 and 20 antenna elements.

anticipate that the bandwidth, B, is a significant fraction of the system operating frequency, f_0. Therefore, the radar is not only operating at the center frequency, but instead all frequencies contained in the interval $f = \left[f_0 - \frac{B}{2}, \quad f_0 + \frac{B}{2}\right]$ are used for transmission. Similar to the previous section, the focus is on a ULA antenna configuration.

The time delay between the sensors, discussed in the previous section, is dependent on the frequency. Therefore, we introduce the phases Φ_l, such that $w_l = e^{-j\Phi_l}$ for the lth antenna element. Thus,

$$\Phi_l = \omega \frac{dl}{c} \sin \alpha. \tag{2.22}$$

In (2.22), $\omega = 2\pi f$ is a frequency contained in the bandwidth of operation, d and α are as before the spacing between adjacent antenna elements and the steering angle, respectively. However, to avoid creating grating lobes, d is typically instead selected as

$$d \leq \frac{c}{2(f_0 + B/2)}. \tag{2.23}$$

Compared with a narrowband antenna array, where only the carrier frequency f_0 is used in operation, if the phases Φ_l in (2.22) are fixed, a change in ω results in a different steering angle, see Figure 2.6. This distortion results in a so-called *beam squinting*. To overcome this distortion, a linear phase filter, i.e., a filter that achieves an approximative constant group delay, is introduced both at the transmit and receive subapertures, which is known as true-time delay technology [1, 13].

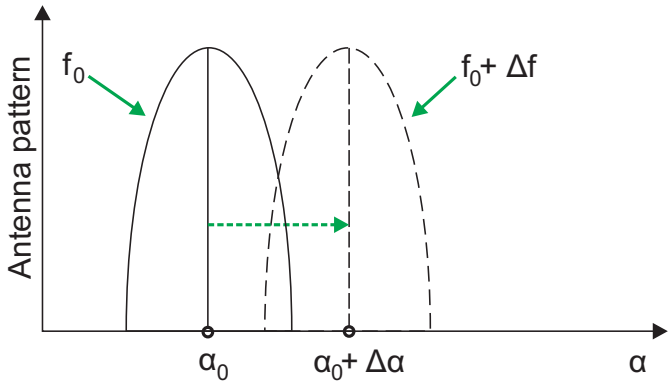

Figure 2.6: Illustration of beam squinting. For fixed phase shifters, a change in frequency affects the steering angle.

Obviously, a narrowband and a wideband ULA produces different array responses. In a 2D space, the wideband array response is, compared with the narrowband array response (2.21), integrated over the bandwidth, which results in

$$\mathrm{AP}(\alpha) = \int_{\omega} \sum_{l=0}^{L-1} \left| e^{-j\omega \frac{dl}{c}(\sin\alpha - \sin\theta)} \right| d\omega. \tag{2.24}$$

Figure 2.7 illustrates the normalized wideband antenna array responses, when the system operates at the carrier frequency $f_0 = 9$ GHz with a bandwidth of $B = \{1, 3, 4\}$ GHz, and an array consisting of $L = 10$ antenna elements. The normalized narrowband and wideband antenna array

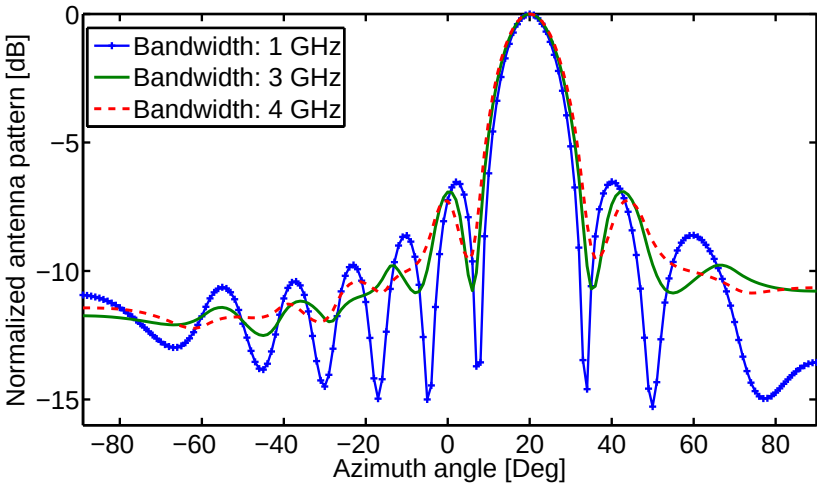

Figure 2.7: Normalized wideband antenna responses utilizing a system bandwidth of $B = \{1, 3, 4\}$ GHz.

responses are illustrated in Figure 2.8. Here, the antenna array still consists

of $L = 10$ elements, the carrier frequency is 9 GHz, and for the wideband case the bandwidth is 2 GHz. As depicted, the narrowband and wideband

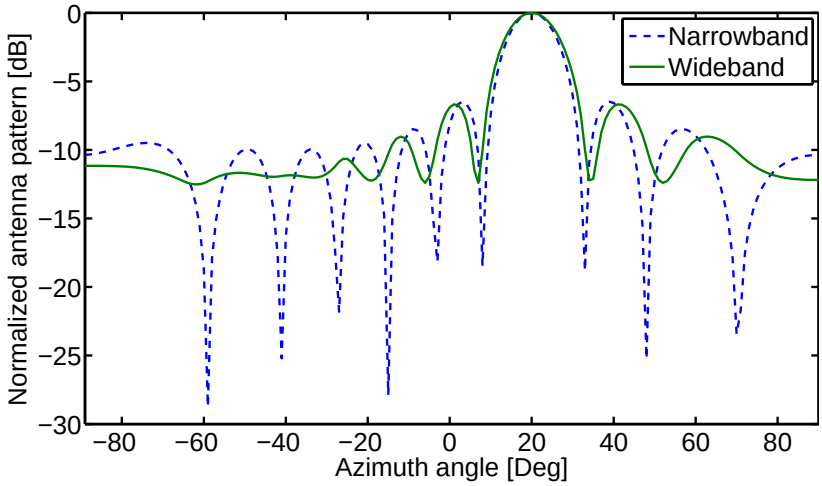

Figure 2.8: Normalized narrowband and wideband antenna array patterns. The graphs are calculated for $L = 10$ elements, $f_0 = 9$ GHz, and $B = 2$ GHz

antenna responses differ from each other, and the difference is greater at larger steering angles. In particular, the depth of the nulls is decreased for the wideband array response.

2.4 Radar Scenario

The radar scenario describes the environment where the radar is operating. In Figure 2.9, an exemplification of a radar scenario is depicted. Clearly, there is not just one scatter point in the environment. In this section, a description of the possible objects is given.

As illustrated, the incoming signal echo does not only contain the desired signal, but also signals from various disturbances, called interference. More precisely, interference is divided into

- clutter
- jamming.

The word clutter refers to returned echoes from undesired objects that naturally appear in the environment. Examples of clutter are: buildings, rain, ground (especially for airborne radar), sea, or animals. Compared with clutter, radar jamming or electronic countermeasures (ECM) are constructed only to interfere with the returns from the desired echo. The ECM is a

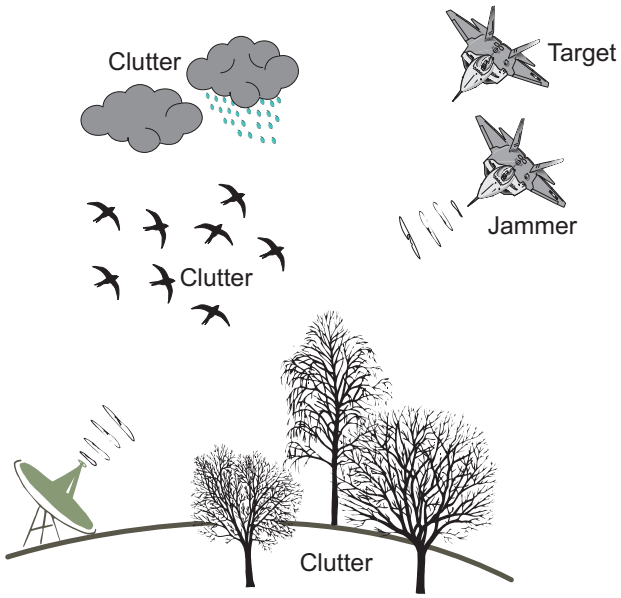

Figure 2.9: Exemplification of a radar scenario comprising a traget and various interference.

part of the radar warfare equipment, which also contains electronic counter-countermeasures and electronic support measures.

There are several different methods of radar jamming, see Figure 2.10 for an overview. As illustrated, jamming is divided into passive and active jamming. The category passive jamming comprises the use of confusing reflectors, such as chaff or reflecting decoys [14], whereas an active jammer deliberately emits electromagnetic radiation to interfere with the returns from the desired echo. Active jamming is divided into noise and deceptive

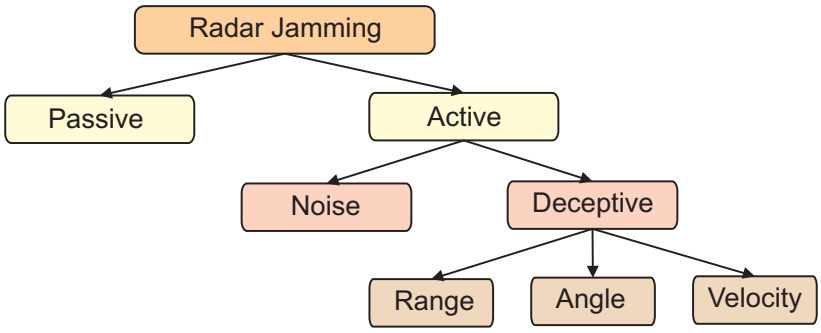

Figure 2.10: Different categories of radar jamming.

jamming, where the noise jammer transmits high power noise to mask the return of the echo. In comparison, a deceptive jammer repeats the transmitted signal with possibly altered angle, velocity, or range [14, 15].

Obviously, when the incoming signal is corrupted by interference, the SNR is not a sufficient measure anymore. Instead, the ratio between the desired signal component and the interference plus noise is of interest. This ratio, called the SNIR, determines the performance of the radar system, and is defined as

$$\text{SNIR} = \frac{P_{\text{signal}}}{P_{\text{noise}} + P_{\text{interference}}}. \tag{2.25}$$

Here, P denotes the average power.

Chapter 3

Robust Transceiver Optimization and Waveform Synthesis

In Chapter 1, it was mentioned that the use of multiple wideband flexible transmitters might significantly increase the performance of future radar systems. We are specifically interested in the improvement in difficult environments, which involve strong clutter and/or jamming. Electronic surveillance equipment with classical libraries of frequencies, pulse repetition intervals, and pulse lengths, may for identification become obsolete, when radar stations are utilizing transmitters with fully adaptive waveforms. It is also anticipated that the optimal waveforms will improve the stealth properties of the radar, i.e., the waveforms will be more difficult to discover compared with the waveforms used nowadays. Our interest is therefore to determine the optimal design of the waveforms to be transmitted.

In this chapter, we introduce the concepts discussed in the appended papers. The overview is divided into three sections. First, in Section 3.1, we give a basic introduction to MIMO radar and waveform design. Thereafter, we describe the concept of designing robust waveforms, see Section 3.2, and finally, the waveform synthesis problem is investigated in Section 3.3. Included in the last section are some new results for the waveform synthesis problem [16].

3.1 MIMO Radar

The interest of MIMO radar originated from the dramatic improvement of MIMO technology in communication systems [3], and the similarities between the two areas are described in [4, 17]. Compared with traditional radar systems, see, e.g., [1, 18], where the antenna elements transmit scaled and either time translated, or phase shifted versions of the signal waveform,

a MIMO radar allows the array elements to transmit arbitrary waveforms. The technique is depicted in Figure 3.1. As shown, each antenna element transmits its own waveform, denoted $x_k(t)$, $k = 1 \dots K$. The received signals $y_l(t)$, $l = 1 \dots L$, are a combination of the back-scattered signals from the target of interest. The transmitted waveforms are either uncorrelated,

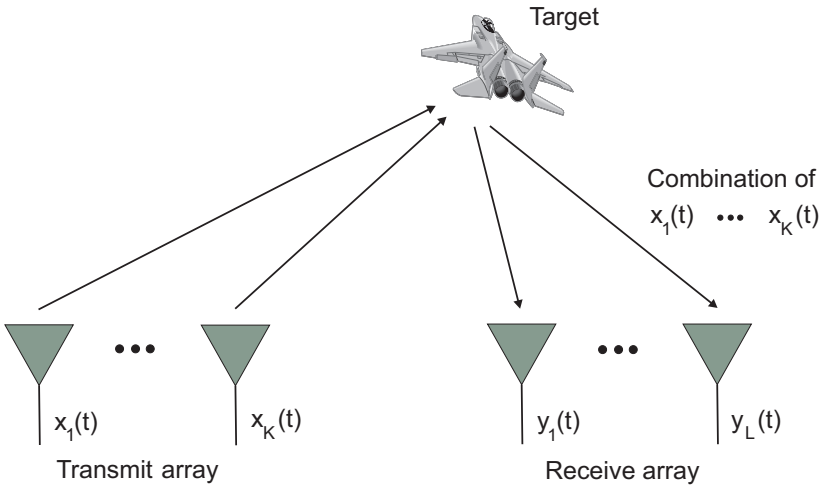

Figure 3.1: MIMO antenna system configuration.

correlated, or partially correlated. In the sequel, we investigate signals that are partially correlated, as the antenna array is to be divided into several subarrays each connected to a waveform generator. Figure 3.1 illustrates a co-located antenna structure, i.e., the antenna elements are closely spaced. This configuration is used throughout this thesis. However, MIMO radar systems are generally divided into employing

- a co-located antenna configuration
- a widely separated antenna configuration.

The diverse configurations enhance different merits of performance. Investigation of widely separated antenna elements shows an increased SNR when exploiting the target's radar cross section [19], improved performance when searching for slowly moving targets [20], and a higher resolution for target localization, as well as the possibility to resolve targets located in the same range cell [5]. In comparison, a co-located antenna configuration likewise offers a higher resolution [4], compared with traditional radar, and an improvement in target identifiability [21].

As we are free to utilize arbitrary waveforms, we seek signals that improve the system performance. In the literature, two design methods are mainly investigated. The first method focuses on the spatial properties of

the transmit signal, see, e.g., [22–25], and the second method concerns the temporal properties of the transmitter–receiver chain, see, e.g., [26–29].

3.1.1 Waveform Design Utilizing the Spatial Properties of the Transmitted Signals

When investigating the spatial properties of the signals, the possibility to optimize the waveforms to coincide with a specific beampattern arises. Assuming a narrowband radar system, the waveform design problem is generally expressed as optimizing the spatial correlations of the waveforms [22,23], where the optimization procedure involves finding the covariance matrix of the waveforms that achieves certain desirable properties. Specifically in [23], four design problems that invoke different design properties are investigated. The investigated problems are

- a maximum power design for unknown target locations
- a maximum power design for known target locations
- a beampattern matching design
- a minimum sidelobe beampattern design.

Obviously, there are many other design problems that have been considered. To incorporate a wideband radar system, the problem is reformulated as the matching of the cross spectral density matrix to a desired spatial beampattern [24]. In [25], the signals are instead described by the Fourier transform of the spatial beampattern. Moreover, an algorithm that performs both the matching of the beampattern and the synthesis of the time domain signals is proposed.

3.1.2 Waveform Design Utilizing the Temporal Properties of the Transmitted Signals

For the second approach, which is investigated in this thesis, a multitude of studies have been performed in the area of MIMO communication, see, e.g., [26–28], where the design of precoders and decoders are discussed. The design of an optimal precoder is addressed in [26], and in [27] the optimal design of space-time precoders and decoders is described. The underlying problems and objectives are quite different for a communication and a radar system. However, the two research areas can still benefit from each other. For example, we use the method proposed by [28] concerning the design of

beamforming weights for complex relay networks, which exploits a predefined power constraint. For radar, the design of transmit and receive filters is discussed in [29], where an alternating method is proposed to increase the SNIR for an extended target in clutter. A similar method is discussed for a single-input multiple-output radar [30, 31], where the SNIR is maximized for a radar scenario containing both target and clutter. In the referenced work, alternating algorithms are proposed that improve the SNIR in each iteration. In [32], instead a gradient based method is proposed, where several suboptimal solutions are studied. The algorithm introduced in [30] can be extended to work for a MIMO system. However, it is not guaranteed that the SNIR increases in each step [29]. In contrast, in [29] a method that works for a MIMO radar system, and which guarantees an increasing SNIR in each iteration, is proposed. The design of adaptive waveforms, where an estimate of the channel statistics is proposed to adapt the transmit signals is discussed in [33]. In [34], robust transmit waveforms and receive filters are studied based on a minimax method. The study is performed for uncertainties related to the target. However, for the proposed algorithms, there is only one power constraint associated with all transmitted waveforms.

Concerning our problem formulation, we are interested in the wideband transmitter–receiver chain depicted in Figure 3.2. The system comprises K

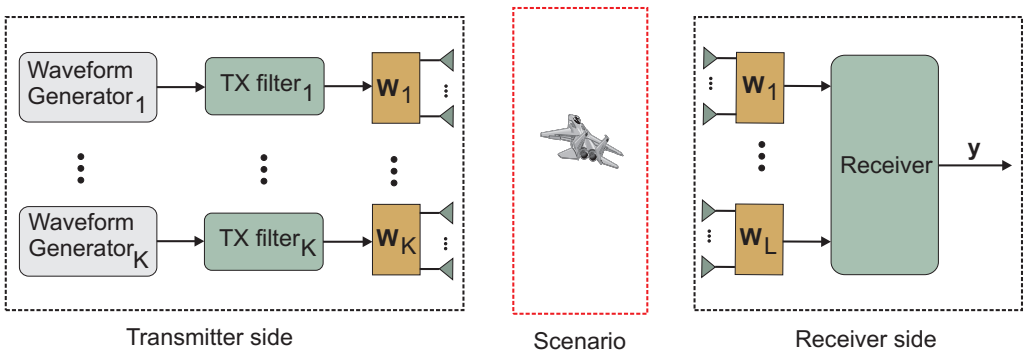

Figure 3.2: Block diagram of the investigated MIMO radar system.

wideband waveform generators, which can produce arbitrary complex signal samples. Obviously, it is possible to design the complete waveforms directly. However, to reduce the system complexity, we introduce one transmit filter for each waveform generator, where the number of filter coefficients, P, are much less than the number of signal samples N. Hence, P complex filter coefficients are derived, instead of N complex signal samples. In this thesis, the transmit filter is modeled as a finite impulse response filter. The wideband antenna array is divided into K subarrays, where each subarray is connected to a transmit filter, and contains K_T antenna elements. Electro-

magnetic waves are emitted from the array, which travel through the radar scenario in the medium of propagation. We discuss a radar scenario that comprises the targets of interest, active jammers, and passive jammers. The main focus is, however, to suppress active jamming interference. Moreover, we do not seek to insert a null in the direction towards such a jammer, as we do not wish the jammer to realize that his position is known. Therefore, to optimize the spatial correlations of the waveforms is not sufficient. The back-scattered echoes from the objects in the environment arrives at the receiver antenna array, which is divided into L subarrays each with L_R antenna elements. We investigate two different receive filter setups. For the first case, the signals are summed and passed through one filter, and in the second case, each subarray is connected to its own receive filter.

The goal is to derive the transmit and receive filter coefficients that maximize the SNIR at the receiver output. The SNIR is expressed in the frequency domain as the obtained power spectral densities (PSDs). Unfortunately, the maximization problem cannot generally be solved in a closed form. The main difference as compared with a MIMO communication system, for which solutions are known [27], is the presence of "intelligent" interference, i.e., deceptive jamming. Therefore, we resort to different attempts to numerically solve the maximization of the SNIR. In Paper 1, we propose two algorithms to derive the transmit and receive filter coefficients: one alternating procedure and one joint optimization method. Note that by joint optimization, we mean that the objective function is reformulated such that it is only dependent on the transmit filter coefficients. Furthermore, two different power constraints on the transmit filters are invoked for both methods, where the first is introduced for all transmit filters and the second for each transmit filter. Thus, we evaluate four maximization problems:

1. An alternating procedure with a total power constraint for all transmit filters.

2. An alternating procedure with individual power constraints for each transmit filter.

3. A joint procedure with a total power constraint for all transmit filters.

4. A joint procedure with individual power constraints for each transmit filter.

To incorporate a total power constraint is of less complexity compared with an individual power constraint, as there are less subsidiary conditions to consider in the optimization. However, the investigation of the individual power constraint is of great importance as large antenna arrays typically

are divided into several subarrays with a power amplifier at each element. Therefore, a power constraint associated with each transmit filter is equivalent to, a power constraint on each antenna element, as the same waveform is used for each element in the subarray.

The steps for the alternating optimization are depicted in Figure 3.3, where the algorithm stops the execution when a specified convergence criterion is satisfied, or when the maximum number of iterations is reached. The convergence criterion used is the difference between the obtained SNIR

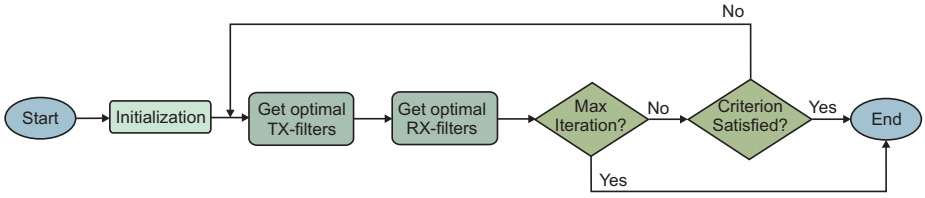

Figure 3.3: Overview of the steps in the alternating optimization.

for two consecutive iterations. The algorithm is initialized with the optimal filter coefficients when no interference is present. To incorporate the different power constraints and receive filter setups, the boxes *Get optimal TX-filters* and *Get optimal RX-filters* contain different functions. This will be further discussed in Paper 1.

3.2 Robust Analysis

In the previous section we introduced the waveform design problem. However, we did not discuss that the positions of the targets and the interference are regarded as known. Thus, we require perfect knowledge of the radar scenario, which generally is not available to the system designer. Consequently, the importance of designing a transmitter–receiver chain that is robust to various imperfections arises.

Robust design methods are a well studied research area, and for an introduction to robust beamforming, see [35] and references therein. In particular, robust methods for parameter estimation, waveform estimation, or beamforming in the presence of model uncertainties for narrowband systems are investigated in [36–38]. For the wideband case, in [39] a robust beamformer is derived based on the approximation of the steering vector by its first order Taylor series expansion [8].

In this report, we investigate two methods to perform the robust design of the transmit filters, namely the waveforms

- a Taylor series expansion

- a worst-case SNIR maximization.

First, if no robust design is imposed, the SNIR reduces dramatically when the position towards the interference is unknown, see Figure 3.4, where σ_s and σ_i are the standard deviation of the target's and interferer's spatial positions, respectively. As illustrated, an uncertainty in the target's position

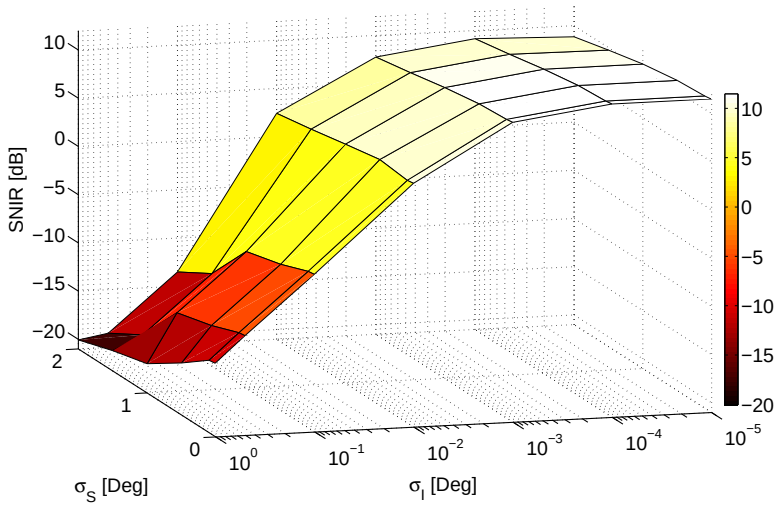

Figure 3.4: The reduction of the SNIR for uncertainties in the target's and the interferer's spatial position.

is not as critical as an uncertainty invoked in the position of the interference. For the first method, we linearize and approximate the SNIR with its second and fourth order Taylor series expansion. Obviously, the fourth order expansion is valid for a larger variance of the spatial position compared with the second order expansion. In the second approach, to solve the worst-case SNIR maximization problem, we propose to use a variation of a minimum-variance distortionless response SNIR maximization. The difference between our approach and the original approach [35, Chapter 2], is that we do not seek beamformers that are robust to pointing errors; instead we seek the robust complex filter coefficients. Hence, the proposed closed-form solution is not applicable when diagonal loading does not apply.

3.3 Waveform Synthesis

In Section 3.1, the design of tunable filters that results in optimal spectral properties for each MIMO channel was discussed. As the radar system performance is directly linked to the time domain characteristics of the

signals, we are interested in how to design the actual time domain signals. Herein, we utilize the obtained spectra to synthesize time domain signals, with desirable properties that coincide with predefined system requirements. The requirements investigated in this thesis are

- a time domain signal with a low PAPR
- a time domain signal with a constant envelope.

The PAPR measures the largest power of a signal sample compared with its average power, and for the sampled signal $\mathbf{y}$, the PAPR is defined as

$$\text{PAPR} = \frac{\max_n |y[n]|^2}{\frac{1}{N}\sum_{n=0}^{N-1} |y[n]|^2}, \tag{3.1}$$

where N is the total number of samples. For a signal with a constant envelope, we require that the PAPR is equal to one. The PAPR is of interest as larger variations require a higher dynamic range on the analog-to-digital converters, as well as power amplifiers with a large linear range. Obviously, this increases the cost and complexity of the radar system.

Schröder [40] studied the problem to synthesize a waveform from a periodic signal with a given power spectrum already in the 70's. He provided formulas to adjust the phase angles, a so-called partial transmit sequence (PTS) technique, of periodic signals that yield a low PAPR, and closed form solutions were derived (for specific power spectra). Continuing, the problem to construct multitone signals with a low PAPR is addressed in [41–43]. Furthermore, in [44] four different PTS based algorithms are discussed, and an extended version of the time–frequency swapping algorithm [43] is selected as the preferred method.

In this thesis, we have investigated two different synthesis methods, where the first invokes a parametrization of the signal in the time domain, and the second instead utilizes a parametrization in the frequency domain. The methods produce two different outcomes:

- A signal with a perfect match of the spectrum with a low PAPR.
- A signal with an imperfect match of the spectrum with a constant envelope.

The first method is discussed in detail in Paper 2, and the results are compared with the preferred time-frequency swapping algorithm in [43]. Hence, in this section we introduce the basics for the second method [16].

To parameterize the signal, we incorporate the discrete Fourier transform (DFT) of a constant envelope signal $Ac[n]$, where A is the amplitude and

$n = 0 \dots N-1$. The total energy in $Ac[n]$ is restricted by Parseval's theorem to

$$\sum_{n=0}^{N-1} |Ac[n]|^2 = \frac{1}{N} \sum_{k=0}^{N-1} |Y_d[k]|^2. \tag{3.2}$$

Here, $|Y_d[k]|^2 = NP_d[k]$, where $P_d[k]$ is the desired spectrum and $k = 0 \dots N-1$. The DFT of $Ac[n]$ is

$$Y[k, \boldsymbol{\phi}] = \sum_{n=0}^{N-1} Ac[n] e^{j\phi_n} e^{-j2\pi \frac{kn}{N}}. \tag{3.3}$$

In (3.3), the introduced phases, $\phi_n \in [0\ 2\pi)$, do not change the implied constant envelope constraint. However, the spectrum changes dramatically with the choice of phases [40]. This is illustrated in Figure 3.5, where the spectra for two different phase dictionaries are depicted. Note that the spectra achieve the same constant magnitude in the time domain. By tuning the phases, ϕ_n, we synthesize a signal with a spectrum that is close to a desired one. Hence, we seek the phases that minimize

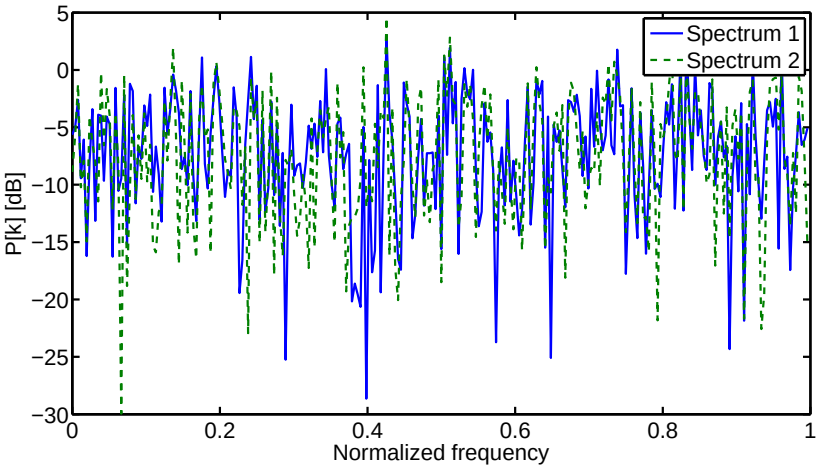

Figure 3.5: Achieved spectra for two different phase dictionaries, $\boldsymbol{\phi}_1$ and $\boldsymbol{\phi}_2$.

$$\hat{\boldsymbol{\phi}} = \arg \min_{\phi_n} \max_{k} f_k(\boldsymbol{\phi}). \tag{3.4}$$

Here, $f_k(\boldsymbol{\phi}) = \left| P[k, \boldsymbol{\phi}] - P_d[k] \right|^2 \cdot w[k]$ is the objective function, $P[k, \boldsymbol{\phi}] = \frac{1}{N}|Y[k, \boldsymbol{\phi}]|^2$, and $\mathbf{w} = \begin{bmatrix} w[1] & \dots & w[N] \end{bmatrix}^T$ is a vector with weight coefficients. The weight function is introduced to emphasize, if necessary, the importance of specific frequency indices. Figure 3.6 illustrates the desired and the obtained spectra after optimization, where the weights are selected

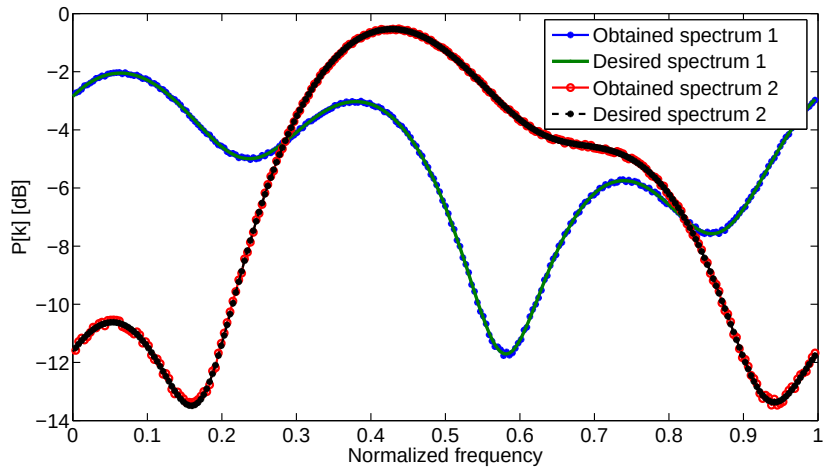

Figure 3.6: Desired and obtained spectra with weights selected as the inverse of the desired power spectrum.

as the inverse of the desired spectrum. Hence, through this normalization, the importance of the low-energy spectral components is increased. As illustrated, the obtained spectra follow the desired ones with very small differences. The weight function is also useful when, for example, we require the spectrum to turn to zero at one or more frequency indices. Assume that we are required to insert a null at the frequency index $k_{\text{notch}} = 128$, with a depth of at least $P_d[k_{\text{notch}}] = -20$ dB. The weight function is set as the inverse of the desired spectrum, and the acquired spectrum is depicted in Figure 3.7.

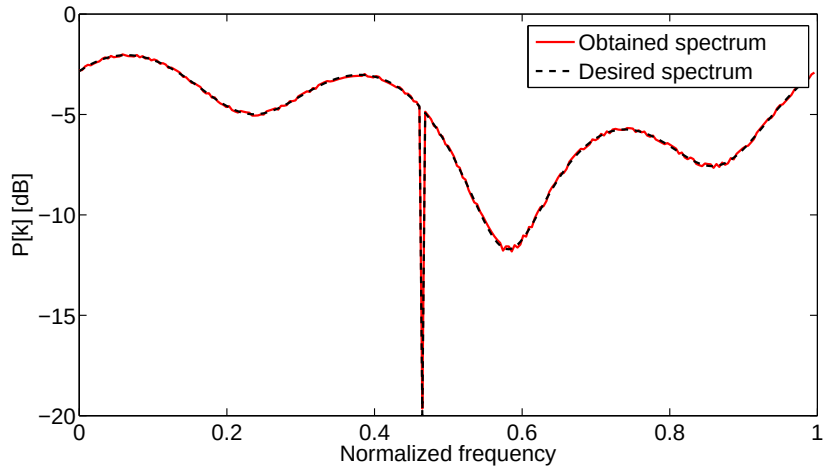

Figure 3.7: Desired and obtained spectra with unequal weights to emphasize the importance of a notch.

Chapter 4

Summary of Appended Papers

This chapter provides a brief summary of the papers that constitute the base for the thesis. Full versions of the papers are included in Part II. The papers have been reformatted to increase readability and to comply with the layout of the rest of the thesis.

Paper 1

> M. Ström, M. Viberg, and K. Falk, Robust Transceiver Design for Wideband MIMO Radar utilizing a Subarray Antenna Structure, To be submitted to *Special Issue on Advances in Sensor Array Processing, EURASIP Signal Processing Journal*.

In this paper, we investigate the possibility to suppress interference for wideband MIMO radar, by exploiting the spectral properties of the transmit signals. We use tunable filters on the transmitter and receiver side, and derive the optimal PSD that enhances the system performance, for a given scenario. Two optimization methods for selecting the optimal transmit and receive filter coefficients are proposed: one alternating and one joint algorithm. Each method is separated into two cases: for a total power constraint and for an individual power constraint on the transmit filters, respectively. The results are extended by introducing a robust design of the transmit filters, where only limited knowledge of the scenario is available. We evaluate two robust design methods: one utilizing the Taylor series expansion of the SNIR and one exploiting a worst-case SNIR maximization.
The analysis in the paper was performed by the thesis author under guidance from the co-authors.

Paper 2

M. Ström and M. Viberg, Low PAPR Waveform Synthesis with Application to Wideband MIMO Radar, *Proc. of the 4th International Workshop on Computational Advances in Multi-Sensor Adaptive Processing* , December 2011, San Juan, Puerto Rico.

Herein, we consider the problem of waveform synthesis given a desired power spectrum. The properties of the designed waveforms are such that the overall system performance is increased. The metric used to evaluate the optimality of the synthesized time domain signals is the PAPR, and the waveforms are synthesized utilizing a PTS based technique. The result is extended by allowing the power spectrum to deviate from its original shape, which yields a further reduction in the PAPR.
The analysis in the paper was performed by the thesis author under guidance from the co-author. This paper has been peer-reviewed. Some minor changes have been made to correct the contents of the paper.

Chapter 5

Conclusions and Future Work

5.1 Conclusions

In this thesis, we investigated two different research problems. The first problem is the design of optimal waveforms for wideband radar systems. The optimality of the waveforms is discussed in terms of the obtained SNIR. We show that it is possible to suppress interference, and especially deceptive jamming interference, by exploiting the temporal properties of the transmitted signals. We advocate the use of tunable filters at the transmitter side to lower the complexity of the system. Hence, instead of deriving the complete signal, only a fraction equal to the number of filter coefficients are derived. The receiver side also employs tunable filters, which are directly given by the signals transmitted in the mainbeam direction.

We formulate two algorithms, where the optimal transmit and receive filters are derived to maximize the SNIR, for a known scenario. The first algorithm invokes an alternating procedure, and the second involves a joint transmit–receive filter optimization. The algorithms are formulated for two different power constraints on the transmit filters: a total and an individual power constraint, respectively. It is seen that a total power constraint is of less complexity compared with an individual power constraint, as there are less subsidiary conditions to consider in the optimization. However, the individual power constraint is of great importance as large antenna arrays typically are divided into several subarrays with a power amplifier at each element. Therefore, a power constraint associated with each transmit filter is equivalent to, a power constraint on each antenna element, as the same waveform is used for each element in the subarray.

Obviously, there is no possibility to acquire perfect knowledge about the radar scenario. Therefore, we extended the results by introducing a robust design of the transmit filters, i.e., the waveforms, for the case where only limited knowledge about the scenario is available. Two robust methods are

reformulated to fit our problem statement, one that is based on the Taylor series expansion of the SNIR, and one that exploits a worse-case SNIR maximization. It is seen that the SNIR is dramatically reduced when the position of the interference is uncertain. However, invoking a robust design leads to a less sensitive system. We propose to use the Taylor series expansion when the mismatch error is relatively low, as it is of less complexity. However, for a larger angular deviation, the Taylor series is not a good approximation, and therefore we need to use the worst-case SNIR maximization.

In the second part of this thesis, we propose a waveform synthesis algorithm that reduces the PAPR for a time domain signal. The designed time domain expression achieves a specific frequency behavior that is agreeable with a desired power spectrum, where the power spectrum is obtained from the optimal waveform design. Our proposed method is compared with the time–frequency swapping method, described in [44], and shows a larger reduction in the PAPR. However, a drawback is that the proposed method is more time consuming. The algorithm is extended by allowing a distortion of the power spectrum. Results show that further reduction of the PAPR is possible, and that the system performance measured as the SNIR is not drastically degraded when allowing small deviations of the power spectra. A variation of the synthesis problem, introduced in Section 3.3, where the time domain signal achieves a constant envelope, whereas the power spectrum instead deviate for its desired shape, is proposed as an alternative. This is so far our preferred method, as the SNIR is not dramatically decreased when the spectrum deviates a small amount from the desired shape.

5.2 Future Work

Our vision is to go towards an adaptive system, where the waveforms constantly adapt to the prevailing conditions. However, there are certain obstacles to overcome before we can make this a reality. First, we need to introduce a time-variant system. Hence, the objects contained in the scenario should move with a velocity at a specific range. Thereafter, we seek to extract information about how the position and the velocity of the interference changes with time. The results are to be used to adapt the waveforms for changes in the position of the interference. Moreover, we seek to evaluate the frequency domain behavior of different kinds of interference, such as clutter and different jammer models.

Furthermore, we wish to combine the results from the transmit and receiver filter optimization with the spatial optimization, and investigate the possible enhancement of performance when both the spatial and temporal

properties of the transmit signals are given a complete freedom.

In this thesis, we have performed an analysis of the robustness to pointing errors. However, this is just one example of the possible sources of error in a radar system. Considering the antenna array, we identify two blocks where errors might occur

- the antenna subarrays
- the antenna elements.

Both the subarrays and the antenna elements in the subarrays experience four types of errors that must be investigated, namely

- phase errors
- amplitude errors
- position errors
- mutual coupling.

We also seek to extend the algorithms to incorporate a 2D antenna array configuration. Another important topic, not discussed in this thesis, is how to evaluate ambiguity issues related to the range and the Doppler.

To continue the work on the waveform synthesis, we seek to constrain both algorithms to consider other system requirements (not only PAPR), for instance, bandwidth and spectral purity. Furthermore, we want to study the degradation in performance when only values contained in a fixed alphabet may be used as phase angles, and not any arbitrary values contained in the interval $\phi_n = (0, 2\pi]$.

References

[1] M. I. Skolnik, *Introduction to radar systems*, 1st ed. McGraw-Hill Int., 1962.

[2] M. A. Richards, *Fundamentals of Radar Signal Processing*, 1st ed. McGraw-Hill Int., 2005.

[3] J. Winters, J. Salz, and R. Gitlin, "The impact of antenna diversity on the capacity of wireless communication systems," *Communications, IEEE Transactions on*, vol. 42, no. 234, pp. 1740 –1751, feb/mar/apr 1994.

[4] D. Bliss and K. Forsythe, "Multiple-input multiple-output (MIMO) radar and imaging: Degrees of freedom and resolution," in *Proc. 37th Asilomar Conf. Signals, Systems and Computers*, November 2003, pp. 54–59.

[5] N. Lehmann, A. Haimovich, R. Blum, and L. Cimini, "High resolution capabilities of MIMO radar," in *Signals, Systems and Computers, 2006. ACSSC '06. Fortieth Asilomar Conference on*, 29 2006-nov. 1 2006, pp. 25 –30.

[6] D. K. Barton, *Modern radar system analysis.* Artech House, Inc., 1988.

[7] S. M. Kay, *Fundamentals of statistical signal processing: detection theory.* Upper Saddle River, NJ, USA: Prentice-Hall, Inc., 1999.

[8] M. Abramowitz and I. A. Stegun, *Handbook of Mathematical Functions with Formulas, Graphs, and Mathematical Tables.* Dover Publications, 1970.

[9] R. J. Mailloux, *Phased Array Antenna Handbook*, 1st ed. Artech House Inc., 1994.

[10] P. S. Naidu, *Sensor Array Signal Processing.* CRC Press, 2000.

[11] H. L. Van Trees, *Optimum Array Processing- Part IV, Detection, Estimation, and Modulation Theory.* John Wiley & Sons, 2002.

[12] H. Krim and M. Viberg, "Two decades of array signal processing research: the parametric approach," *Signal Processing Magazine, IEEE*, vol. 13, no. 4, pp. 67 –94, jul 1996.

[13] I. Frigyes and A. Seeds, "Optically generated true-time delay in phased-array antennas," *Microwave Theory and Techniques, IEEE Transactions on*, vol. 43, no. 9, pp. 2378 –2386, sep 1995.

[14] R. N. Lothes, M. B. Szymanski, and R. G.Wiley, *Radar vulnerability to jamming.* Artech House, 1990.

[15] L. Neng-Jing and Z. Yi-Ting, "A survey of radar ECM and ECCM," *Aerospace and Electronic Systems, IEEE Transactions on*, vol. 31, no. 3, pp. 1110 –1120, jul 1995.

[16] M. Ström and M. Viberg, "Constant modulus waveform synthesis with application to wideband MIMO radar," in *presented at the Swedish Radio and Microwave Days*, Stockholm, Sweden, 2012.

[17] E. Fishler, A. Haimovich, R. Blum, D. Chizhik, L. Cimini, and R. Valenzuela, "MIMO radar: an idea whose time has come," in *Proc. of the IEEE Int. Conf. on Radar*, Philadelphia, PA, April 2004.

[18] D. E. Vakman, *Sophisticated Signals and the Uncertainty Principle in Radar.* Springer Verlag Berlin, 1968.

[19] E. Fishler, A. Haimovich, R. Blum, J. Cimini, L.J., D. Chizhik, and R. Valenzuela, "Spatial diversity in radars-models and detection performance," *Signal Processing, IEEE Transactions on*, vol. 54, no. 3, pp. 823 – 838, march 2006.

[20] Q. He, N. H. Lehmann, R. S. Blum, and A. M. Haimovich, "MIMO radar moving target detection in homogeneous clutter," *Aerospace and Electronic Systems, IEEE Transactions on*, vol. 46, no. 3, pp. 1290 –1301, july 2010.

[21] J. Li, P. Stoica, L. Xu, and W. Roberts, "On parameter identifiability of MIMO radar," *Signal Processing Letters, IEEE*, vol. 14, no. 12, pp. 968 –971, dec. 2007.

[22] D. R. Fuhrmann and G. S. Antonio, "Transmit beamforming for MIMO radar systems using partial signal correlations," in *38th Asilomar Conference on Signals, Systems and Computers*, Pacific Grove, CA, November 2004.

[23] J. Li, P. Stoica, and Y. Xie, "On probing signal design for MIMO radar," *IEEE Trans. on Sig. Process.*, vol. 55, pp. 4151–4161, August 2007.

[24] G. S. Antonio and D. Fuhrmann, "Beampattern synthesis for wideband MIMO radar systems," in *The first IEEE Int. workshop on Comp. Advances in Multi-Sensor Adaptive processing*, Puerto Vallarta, Mexico, December 2005, pp. 105–108.

[25] H. Hao, P. Stoica, and L. Jian, "Wideband MIMO systems: signal design for transmit beampattern synthesis," *IEEE Trans. on Sig. Proc.*, vol. 59, pp. 618–628, February 2011.

[26] L. Collin, O. Berder, P. Rostaing, and G. Burel, "Optimal minimum distance-based precoder for MIMO spatial multiplexing systems," *Signal Processing, IEEE Transactions on*, vol. 52, no. 3, pp. 617 – 627, march 2004.

[27] A. Scaglione, P. Stoica, S. Barbarossa, G. B. Giannakis, , and H. Sampat, "Optimal designs for space time linear precoders and decoders," *IEEE Trans. on Sig. Proc.*, vol. 50, pp. 1051–1064, May 2002.

[28] V. Havary-Nassab, S. Shahbazpanahi, A. Grami, and Z. Luo, "Distributed beamforming for relay networks based on second-order statistics of the channel state information," *IEEE Trans. on Sig. Proc.*, vol. 56, pp. 4306–4316, September 2008.

[29] C. Chen and P. P. Vaidyanathan, "MIMO radar waveform optimization with prior information of extended target and clutter," *IEEE Trans. on Sig. Proc.*, vol. 57, pp. 3533–2543, September 2009.

[30] S. Pillai, H. Oh, D. Youla, and J. Guerci, "Optimal transmit-receiver design in the presence of signal-dependent interference and channel noise," *Information Theory, IEEE Transactions on*, vol. 46, no. 2, pp. 577 –584, mar 2000.

[31] D. DeLong and E. Hofstetter, "On the design of optimum radar waveforms for clutter rejection," *Information Theory, IEEE Transactions on*, vol. 13, no. 3, pp. 454 –463, july 1967.

[32] B. Friedlander, "Waveform design for MIMO radars," *Aerospace and Electronic Systems, IEEE Transactions on*, vol. 43, no. 3, pp. 1227 –1238, july 2007.

[33] J. Guerci, M. Wicks, J. Bergin, P. Techau, and S. Pillai, "Theory and application of optimum and adaptive mimo radar," in *Radar Conference, 2008. RADAR '08. IEEE*, may 2008, pp. 1 –6.

[34] B. Jiu, H. Liu, D. Feng, and Z. Liu, "Minimax robust transmission waveform and receiving filter design for extended target detection with imprecise prior knowledge," *Signal Processing*, vol. 92, no. 1, pp. 210 – 218, 2012.

[35] J. Li and P. Stoica, *Robust adaptive beamforming*. John Wiley and Sons, Inc., 2006.

[36] S. Vorobyov, A. Gershman, and Z.-Q. Luo, "Robust adaptive beamforming using worst-case performance optimization: a solution to the signal mismatch problem," *Signal Processing, IEEE Transactions on*, vol. 51, no. 2, pp. 313 – 324, feb 2003.

[37] O. Besson, A. Monakov, and C. Chalus, "Signal waveform estimation in the presence of uncertainties about the steering vector," *Signal Processing, IEEE Transactions on*, vol. 52, no. 9, pp. 2432 – 2440, sept. 2004.

[38] Y. Yang and R. Blum, "Minimax robust MIMO radar waveform design," *Selected Topics in Signal Processing, IEEE Journal of*, vol. 1, no. 1, pp. 147 –155, june 2007.

[39] M. Er and B. Ng, "A robust method for broadband beamforming in the presence of pointing error," *Signal Processing*, vol. 30, no. 1, pp. 115 – 121, 1993.

[40] M. R. Schroeder, "Synthesis of low-peak-factor signals and binary sequences with low autocorrelation," *IEEE Trans. Inform. Theory*, vol. IT-16, pp. 85–89, January 1970.

[41] S. Boyd, "Multitone signals with low crest factor," *IEEE Trans. Circuits and Syst.*, vol. 33, no. 10, pp. 1018 – 1022, oct 1986.

[42] A. Van Den Bos, "A new method for synthesis of low-peak-factor signals," *IEEE Trans. Acoust., Speech Signal Process.*, vol. 35, no. 1, pp. 120 – 122, jan 1987.

[43] E. Van der Ouderaa, J. Schoukens, and J. Renneboog, "Peak factor minimization of input and output signals of linear systems," *IEEE Trans. Instrum. Meas.*, vol. 37, no. 2, pp. 207 –212, jun 1988.

[44] M. Friese, "Multitone signals with low crest factor," *IEEE Trans. Commun.*, vol. 45, no. 10, pp. 1338 –1344, oct 1997.

Part II

Included Papers